Theory of the cyclotron resonance spectrum of a polaron in two dimensions

Wu Xiaoguang, F. M. Peeters, and J. T. Devreese*
University of Antwerp (Universitaire Instelling Antwerpen), Department of Physics, Universiteitsplein 1, B-2610 Wilrijk-Antwerpen, Belgium
(Received 2 June 1986)

The magneto-optical absorption spectrum of a two-dimensional polaron is calculated by using a memory-function approach. The cyclotron resonance frequency and the cyclotron resonance mass of the polaron are obtained for weak electron-phonon coupling. The absorption spectrum exhibits peaks around the cyclotron frequency ω_c and the LO-phonon-assisted harmonics $\omega_{LO}+n\omega_c$ ($n=1,2,\ldots$). The oscillator strength and the position of the peaks are investigated as a function of the magnetic field strength. A Landau-level broadening parameter is introduced phenomenologically in order to remove the divergencies in the magneto-optical absorption spectrum. The effect of the nonzero width of the two-dimensional electron layer is also investigated. After taking into account the effect of the nonparabolic energy band of the electron, the calculated cyclotron resonance masses are compared to the experimental data for GaAs-$Al_xGa_{1-x}As$ heterostructures and InSb inversion layers. In order to explain the experimental results for GaAs-$Al_xGa_{1-x}As$ heterostructures with our one polaron theory an *effective* electron-phonon coupling constant has to be used which is smaller than generally accepted. Many-body effects are expected to be responsible for this reduction.

I. INTRODUCTION

In polar semiconductors and ionic crystals an electron interacts with longitudinal-optical (LO) phonons. In the presence of a magnetic field there will be so-called *resonant polaron effects* when ω_c, the unperturbed cyclotron frequency, approaches ω_{LO}, the LO-phonon frequency. The main evidence for the existence of resonant polaron effects is provided by a cyclotron-resonance experiment. In such an experiment the mass renormalization of the electron due to the polaron effect is observed clearly. Over the last few decades three-dimensional (3D) polarons have been extensively studied. For a review of the theoretical and experimental progress in this field, we refer to Ref. 1.

Recently, due to technological progress in material growth (e.g., the advent of molecular-beam epitaxy), quasi-two-dimensional (Q2D) electron systems have been created in polar semiconductors. Examples of such systems are GaAs-$Al_xGa_{1-x}As$ heterostructures, $Ga_{1-x}In_xAs$ heterojunctions, InSb inversion layers, etc.[2] Only very recently have polaron effects been studied in these 2D systems.[3-12] The main emphasis was on the investigation of the peak position of the cyclotron-resonance line and on the splitting of the line around the resonance frequency $\omega_c=\omega_{LO}$. In Ref. 8, by using a Green's-function approach, Das Sarma and Madhukar made a formal calculation to investigate the Landau-level correction and the magneto-optical anomalies in the resonant region. They showed that the influence of the electron-phonon coupling in 2D systems can lead to a splitting of the cyclotron-resonance line when $\omega_c\sim\omega_{LO}$, which is similar to that for the 3D polaron (see, for instance, Ref. 13 and references therein). In their calculation off-resonance terms in the perturbation theory were neglected. Subsequently, Larsen studied the cyclotron resonance of a 2D polaron using the Rayleigh-Schrödinger perturbation theory (RSPT).[9] In Ref. 9 the effect due to the nonzero density of the electron gas on the polaron Landau levels was also investigated by summing the most divergent terms in the perturbation theory to all orders. The electron-phonon interaction correction to the Landau levels of the 2D polaron has also been studied by the present authors using the so-called improved Wigner-Brillouin perturbation theory (IWBPT).[10] Most of the above-mentioned studies are based on a perturbation calculation of the position of the Landau levels of the 2D polaron. The cyclotron-resonance mass of the electron is then obtained from the difference in energy between two adjacent Landau levels.

In this paper we present a calculation of the 2D polaron cyclotron resonance spectrum which is based on a memory-function approach.[13-16] Instead of calculating polaron energy levels, we calculate the magneto-optical absorption spectrum, which is expressed in terms of a memory function. Our motivation is that the magneto-optical absorption is the physical measured quantity. The cyclotron-resonance frequency and the cyclotron-resonance mass of the electron are obtained from the position of certain peaks in the magneto-optical absorption spectrum. The present paper is divided into two parts: The first part contains our theoretical calculation, and in the second part our results are compared with recent experimental data.[4-6]

In the theoretical part of this paper we limit ourselves to a single electron with a parabolic energy band, interacting with bulk LO phonons. The effect of the nonzero width of the 2D electron layer is included by considering the lowest subband where the standard variational wave function is used.[2] We also introduce a Landau-level broadening parameter[2,16] in order to remove the divergencies in the absorption spectrum. This is equivalent to a standard procedure in which the unperturbed density of states, which consists of a series of δ functions, is replaced

 ©1986 The American Physical Society

by a set of Gaussian functions. The electron-phonon interaction is treated as a perturbation and the memory function is calculated to first order in the electron-phonon coupling constant. The spin, the effect resulting from Fermi-Dirac statistics, and the screening effect of the electron gas are neglected in the present study.

The present paper is organized as follows: In Sec. II we outline the calculation of the memory function including the effect of the finite width of the 2D electron layer and of the Landau-level broadening. The magneto-optical absorption spectra of the 2D polaron are then calculated. Section III contains our numerical results and discussion. In Sec. IV we take into account the band nonparabolicity and compare our calculations with recent experimental data. Our conclusion is presented in Sec. V.

II. FORMULATION AND CALCULATION

The electron-phonon system is described by the Fröhlich Hamiltonian

$$\mathcal{H}=\frac{1}{2m_b}\left[\mathbf{p}+\frac{e\mathbf{A}}{c}\right]^2+\sum_{\mathbf{k}}\hbar\omega_{\mathrm{LO}}a_{\mathbf{k}}^{\dagger}a_{\mathbf{k}}+\sum_{\mathbf{k}}(V_{\mathbf{k}}a_{\mathbf{k}}e^{i\mathbf{k}\cdot\mathbf{r}}+V_{\mathbf{k}}^{*}a_{\mathbf{k}}^{\dagger}e^{-i\mathbf{k}\cdot\mathbf{r}}) , \tag{1}$$

where $\mathbf{p}$ ($\mathbf{r}$) is the momentum (position) operator of an electron. $a_{\mathbf{k}}^{\dagger}$ ($a_{\mathbf{k}}$) is the creation (annihilation) operator of a bulk LO phonon with wave vector $\mathbf{k}$ and energy $\hbar\omega_{\mathrm{LO}}$. The magnetic field H is taken perpendicular to the 2D electron layer and the z axis is chosen along the direction of the magnetic field. In Eq. (1) $V_{\mathbf{k}}$ is given by

$$V_{\mathbf{k}}=i\hbar\omega_{\mathrm{LO}}\left[\frac{4\pi\alpha}{Vk^2}\right]^{1/2}\left[\frac{\hbar}{2m_b\omega_{\mathrm{LO}}}\right]^{1/4}\langle\psi_0|e^{ik_z z}|\psi_0\rangle , \tag{2}$$

where $\psi_0(z)=(b^3/2)^{1/2}ze^{-bz/2}$ is the variational wave function describing the motion of the electron in the direction normal to the 2D electron layer. b is given by

$$b=(48\pi Nm_b e^2/\hbar^2\epsilon_0)^{1/3} ,$$

where $N=n_d+\frac{11}{32}n_e$ and n_d and n_e are the depletion and carrier charge density, respectively. For simplicity we take into account only the lowest subband and neglect all higher subbands. Such an approximation results in Eq. (2).

Within linear-response theory the dynamical conductivity of the system can be written as

$$\sigma(\omega)=\frac{in_e e^2/m_b}{\omega-\omega_c-\Sigma(\omega)} , \tag{3}$$

where $\Sigma(\omega)=\Sigma(\alpha,\omega_c,b;\omega)$ is the memory function.[13–16] $\omega_c=eH/m_bc$ is the cyclotron resonance frequency when no polaron effects are present. The magneto-optical absorption is defined as the real part of Eq. (3) (within a factor)

$$\frac{-\mathrm{Im}\Sigma(\omega)}{[\omega-\omega_c-\mathrm{Re}\Sigma(\omega)]^2+[\mathrm{Im}\Sigma(\omega)]^2} . \tag{4}$$

The zero-magnetic-field limit of Eq. (4) leads to an expression similar to that obtained in Ref. 16. In the present paper the memory function will be calculated within an approximation similar to that used in Ref. 15. This amounts to a perturbational calculation of $\Sigma(\omega)$. To first order in the electron-phonon coupling constant the memory function has the form (see also Refs. 16 and 18 for the zero-magnetic-field case)

$$\Sigma(\omega)=\frac{1}{\omega}\int_0^{\infty}dt(1-e^{i\omega t})\mathrm{Im}F(t) , \tag{5a}$$

and

$$F(t)=-\sum_{\mathbf{k}}\frac{k_{\parallel}^2}{m_b\hbar}|V_{\mathbf{k}}|^2\{[1+n(\omega_{\mathrm{LO}})]\langle e^{i\mathbf{k}\cdot\mathbf{r}(t)}e^{-i\mathbf{k}\cdot\mathbf{r}(0)}\rangle-n(\omega_{\mathrm{LO}})\langle e^{-i\mathbf{k}\cdot\mathbf{r}(0)}e^{i\mathbf{k}\cdot\mathbf{r}(t)}\rangle\}e^{-i\omega_{\mathrm{LO}}t} , \tag{5b}$$

where $n(\omega_{\mathrm{LO}})=(e^{\beta\hbar\omega_{\mathrm{LO}}}-1)^{-1}$ is the number of phonons and $k_{\parallel}^2=k_x^2+k_y^2$. $\langle\ \rangle$ stands for the average and must be calculated without electron-phonon interaction in order to be consistent with the memory-function calculation.

The problem is now reduced to the calculation of a density-density correlation function

$$I(\mathbf{k},t)=\langle e^{i\mathbf{k}\cdot\mathbf{r}(t)}e^{-i\mathbf{k}\cdot\mathbf{r}(0)}\rangle . \tag{6}$$

In the following we will concentrate on the zero-temperature case and calculate $I(\mathbf{k},t)$ to zero order in the electron-phonon interaction, which amounts to a replacement of the Hamiltonian $\mathcal{H}$ by $\mathcal{H}_0$ ($\mathcal{H}_0$ is the Hamiltonian of a free electron in a magnetic field). The calculation of $I(\mathbf{k},t)$ is analogous to a similar calculation given in Ref. 10. Here we give the main steps

$$\begin{aligned}I(\mathbf{k},t)&=\sum_n\langle 0|e^{i\mathcal{H}_0t/\hbar}|0\rangle\langle 0|e^{i\mathbf{k}\cdot\mathbf{r}}|n\rangle\langle n|e^{-i\mathcal{H}_0t/\hbar}|n\rangle\langle n|e^{-i\mathbf{k}\cdot\mathbf{r}}|0\rangle\\&=\sum_n e^{iE_0t/\hbar-\Gamma^2t^2/8}\langle 0|e^{i\mathbf{k}\cdot\mathbf{r}}|n\rangle e^{-iE_nt/\hbar-\Gamma^2t^2/8}\langle n|e^{-i\mathbf{k}\cdot\mathbf{r}}|0\rangle\\&=e^{-\Gamma^2t^2/4}\sum_n e^{iE_0t/\hbar}\langle 0|e^{i\mathbf{k}\cdot\mathbf{r}}|n\rangle e^{-iE_nt/\hbar}\langle n|e^{-i\mathbf{k}\cdot\mathbf{r}}|0\rangle\\&=e^{-\Gamma^2t^2/4}\exp\left[-\frac{\hbar k^2}{2m_b\omega_c}(1-e^{-i\omega_ct})\right] ,\end{aligned} \tag{7}$$

where $|n\rangle$ is the wave function of the unperturbed nth Landau level. In Eq. (7) we introduce the Landau-level broadening parameter Γ by assuming that the propagator of a free electron is $\exp(-iE_n t/\hbar-\Gamma^2 t^2/8)$ (see Refs. 2 and 17). For convenience we choose Γ independent of the Landau-level number.

After some algebra we arrive at

$$F(t)=\eta\int_0^\infty dx\, x^2 f(x,b_0)\times\exp\left[-x^2(1-e^{-i\omega_c t})-\frac{\Gamma^2 t^2}{4}-i\omega_{\rm LO}t\right], \tag{8}$$

where $\eta=2\alpha\omega_{\rm LO}^3(\omega_c/\omega_{\rm LO})^{3/2}$ and $b_0=b(\hbar/2m_b\omega_c)^{1/2}$. The form factor $f(k,b)$ is given by

$$f(k,b)=(8b^3+9b^2k+3bk^2)/[8(b+k)^3]$$

which expresses the nonzero width of the 2D electron layer.

The explicit form of the memory function can be obtained from Eqs. (5). In the present paper we will give numerical results for the case of zero lattice temperature. In this limit the real part of the memory function becomes

$$\mathrm{Re}\Sigma(\omega)=\sum_{n=0}^{\infty}\frac{B_n}{\omega\Gamma}\left[2D\left[\frac{\varepsilon_n}{\Gamma}\right]-D\left[\frac{\varepsilon_n+\omega}{\Gamma}\right]-D\left[\frac{\varepsilon_n-\omega}{\Gamma}\right]\right], \tag{9a}$$

and the imaginary part

$$\mathrm{Im}\Sigma(\omega)=\sum_{n=0}^{\infty}\frac{\sqrt{\pi}B_n}{2\omega\Gamma}\left[\exp\left[-\frac{(\varepsilon_n+\omega)^2}{\Gamma^2}\right]-\exp\left[-\frac{(\varepsilon_n-\omega)^2}{\Gamma^2}\right]\right], \tag{9b}$$

with

$$B_n=\frac{\eta}{n!}\int_0^\infty dx\, x^2 f(x,b_0)x^{2n}e^{-x^2}, \tag{9c}$$

where $\varepsilon_n=\omega_{\rm LO}+n\omega_c$ and

$$D(t)=e^{-t^2}\int_0^t dx\, e^{x^2}$$

is the Dawson integral. The real and imaginary parts of the memory function given by Eqs. (9a) and (9b) satisfy the Kramers-Kronig relation

$$\mathrm{Re}\Sigma(\omega)=-\frac{1}{\pi}\int_{-\infty}^{+\infty}dx\frac{\mathrm{Im}\Sigma(x)}{\omega-x}, \tag{10}$$

where the integral is interpreted as a principal integration.

III. NUMERICAL RESULTS AND DISCUSSION

We have performed the numerical calculation of the memory function and of the magneto-optical absorption spectrum. First, we study the case with zero Landau-level broadening, i.e., $\Gamma=0$. In this case the imaginary part of the memory function consists of a series of δ functions at the frequencies $\omega=\omega_{\rm LO}+n\omega_c$ ($n=0,1,2,\ldots$). The real part of the memory function diverges at $\omega=\omega_{\rm LO}+n\omega_c$ as $1/(\omega-\omega_{\rm LO}-n\omega_c)$ [see Eq. (9a)]. Due to this special structure of the imaginary part of the memory function the magneto-optical absorption spectrum consists of a series of δ-function peaks. The position of these peaks are determined by the equation $\omega-\omega_c-\mathrm{Re}\Sigma(\omega)=0$ and are thus not influenced by the imaginary part of the memory function. The δ-function peaks in the absorption spectrum have oscillator strength

$$\pi\left[1-\frac{\partial}{\partial\omega}\mathrm{Re}\Sigma(\omega)\right]^{-1}.$$

In Fig. 1 the frequencies (ω^*) of the first four peaks in the magneto-optical absorption spectrum are plotted as a function of the magnetic field for an ideal 2D system. These peaks correspond to the transitions of the polaron from the ground state ($n=0$) to the nth ($n=1,2,3$) Landau level. The splitting of ω_1^* and ω_2^* around $\omega_c=\omega_{\rm LO}$, and the pinning behavior of ω_2^* for $\omega_c\gg\omega_{\rm LO}$, are clearly seen from this figure. In Ref. 19 a detailed comparison was made between the results of the IWBPT calculation and the present results. It was suggested in Ref. 19 that the present approach is a rather good approximation in calculating the polaron cyclotron-resonance mass, even for $\alpha\sim 0.1$.

We compare the ideal 2D and Q2D results in Fig. 2. The effective mass of the electron, which is derived from

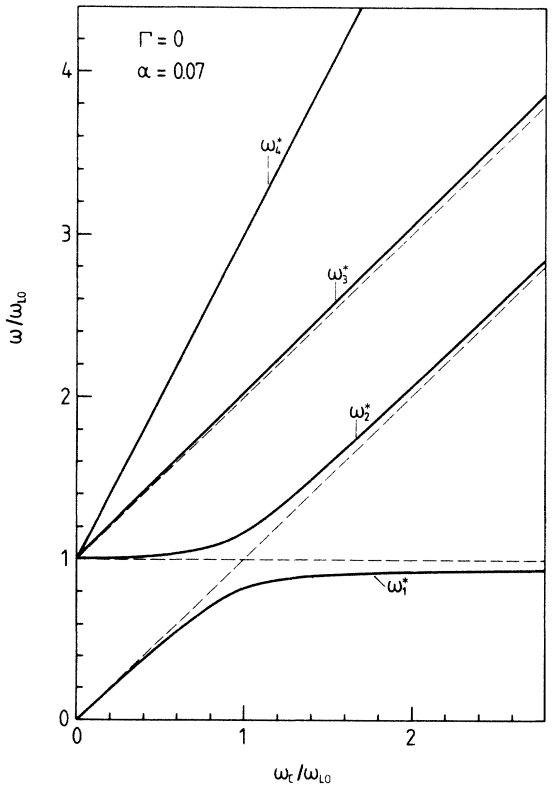

FIG. 1. The positions of the first four peaks in the magneto-optical absorption spectrum are plotted as a function of the magnetic field strength for an ideal 2D system.

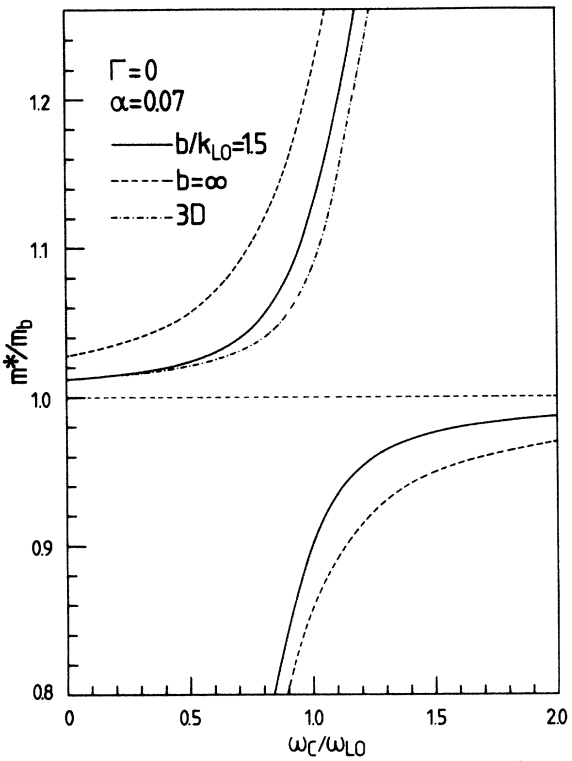

FIG. 2. The cyclotron-resonance mass derived from the magneto-optical absorption spectrum is shown as a function of the magnetic field for the 2D and Q2D systems. The 3D result is given by the dash-dotted curve.

ω_1^* and ω_2^* by $m^*=\omega_c/\omega_1^*$ for $\omega_c<\omega_{LO}$ and $m^*=\omega_c/\omega_2^*$ for $\omega_c>\omega_{LO}$, is plotted as a function of the magnetic field strength. As for the zero-magnetic-field case,[20] the nonzero width of the electron layer reduces the polaron effects. This reduction is a consequence of the fact that the form factor $f(k,b)\leq 1$ in Eq. (9), while for the ideal 2D system $f(k,b=\infty)=1$. Notice that the splitting of the first two Landau levels is not symmetrical about the LO-phonon energy, i.e., $\omega_{LO}-\omega_1^*\neq\omega_2^*-\omega_{LO}$, at $\omega_c=\omega_{LO}$. A similar result was recently found for the IWBPT theory.[10] In Fig. 2 we also plot the corresponding 3D results for $\omega^*<\omega_{LO}$ (for $\omega^*>\omega_{LO}$ the situation is more complicated since the imaginary part of the memory function is different from zero[13]). For the ideal 2D system the polaron effect is enhanced compared to the 3D case, i.e., we have a larger polaron-mass correction. For the zero-magnetic-field case a similar result was found earlier.[20] In the zero-magnetic-field limit we find the familiar result $m^*/m_b=1+\pi\alpha/8$ for the ideal 2D system.

The oscillator strength of the first four δ-function peaks is plotted as a function of the magnetic field for the ideal 2D and Q2D systems in Fig. 3(a) and Fig. 3(b), respectively. The nonzero width of the 2D electron layer does not change the qualitative behavior of the oscillator strength. Most of the oscillator strength is contained in the first two peaks. As the magnetic field increases, the oscillator strength is transferred from the first cyclotron-resonance peak to the second peak. For the Q2D system such a transfer of the oscillator strength is more abrupt

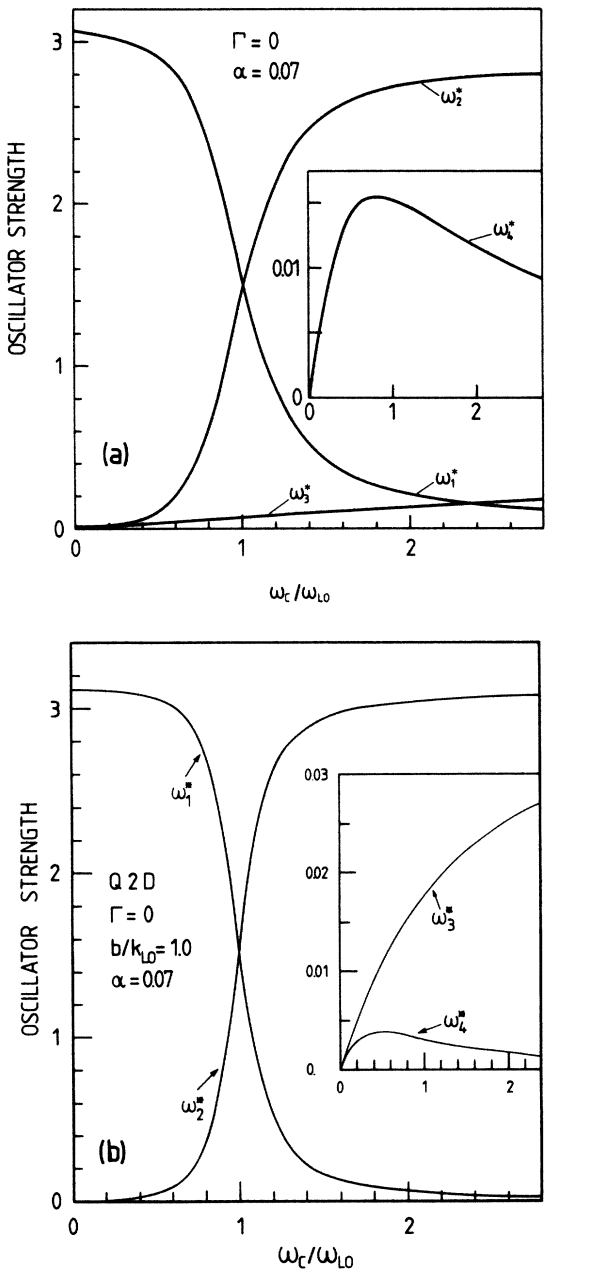

FIG. 3. The oscillator strength of the first four δ-function peaks in the magneto-optical absorption spectrum is shown as a function of the magnetic field for (a) the ideal 2D system and (b) for the Q2D system.

due to the reduction of the polaron effects [see Fig. 3(b)]. From Fig. 3 we can conclude that the oscillator strength of the nth LO-phonon-assisted harmonic is roughly an order of magnitude smaller than the oscillator strength of the $(n-1)$th LO-phonon assisted harmonic. Furthermore, note the interesting result that the oscillator strength of ω_3^* increases with increasing magnetic field, while for ω_4^* it increases up to $\omega_c\sim\omega_{LO}/2$ and starts to decrease for larger magnetic fields. The behavior of the oscillator strength found here are similar to that found for the 3D polaron.[1]

In Fig. 4 the cyclotron-resonance mass of the electron

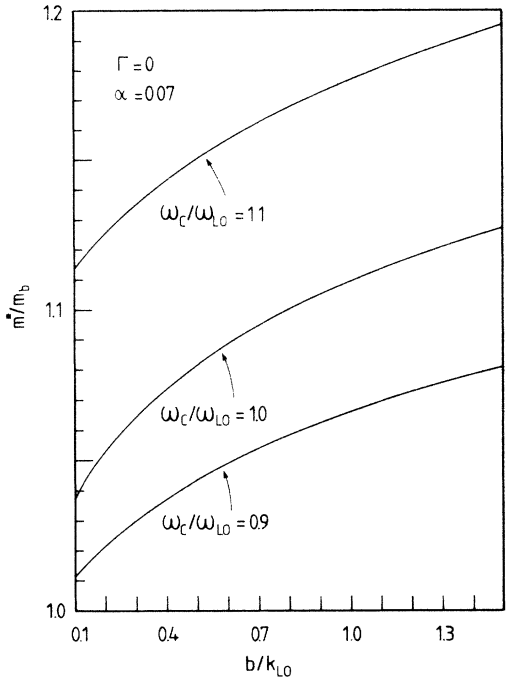

FIG. 4. The cyclotron-resonance mass derived from the first peak of the magneto-optical absorption spectrum is shown as a function of b for different values of the magnetic field.

derived from the first peak is plotted as a function of b, which is inversely proportional to the width of the 2D electron layer, for different values of the magnetic field. As b increases the 2D electron layer becomes narrower and closer to the ideal 2D system. Consequently, the effective electron-phonon coupling strength is enhanced and the polaron correction to the cyclotron-resonance mass of the electron increases as shown in Fig. 4. We point out that in the limit of $b \to 0$ we do not recover the 3D results. This is due to the fact that in the present study we only consider the lowest subband.

In the case $\Gamma > 0$ the Landau levels have a nonzero width and the real and imaginary parts of the memory function are continuous functions of the frequency. All δ-function peaks in the absorption spectrum are broadened. In this case the position of a peak is determined by the maximum in the absorption spectrum, which is determined by the behavior of $\mathrm{Re}\Sigma(\omega)$ and $\mathrm{Im}\Sigma(\omega)$. These peaks do not necessarily coincide with the zeros of $\omega - \omega_c - \mathrm{Re}\Sigma(\omega) = 0$. In the present study the Landau-level broadening parameter is introduced phenomenologically and taken as a given constant. The broadening of the Landau levels may be attributed to impurity scattering, electron-electron interaction, higher orders of the electron LO-phonon interaction, acoustic-phonon scattering, etc.[2]

The real and imaginary parts of the memory function are plotted in Figs. 5(a) and 5(b), respectively, for the ideal 2D system. The imaginary part of the memory function consists of a series of peaks around $\omega = \omega_{\mathrm{LO}} + n\omega_c$ ($n = 0, 1, 2, \ldots$). The amplitude of the peaks decreases with increasing n. This can be seen from Eqs. (9) because

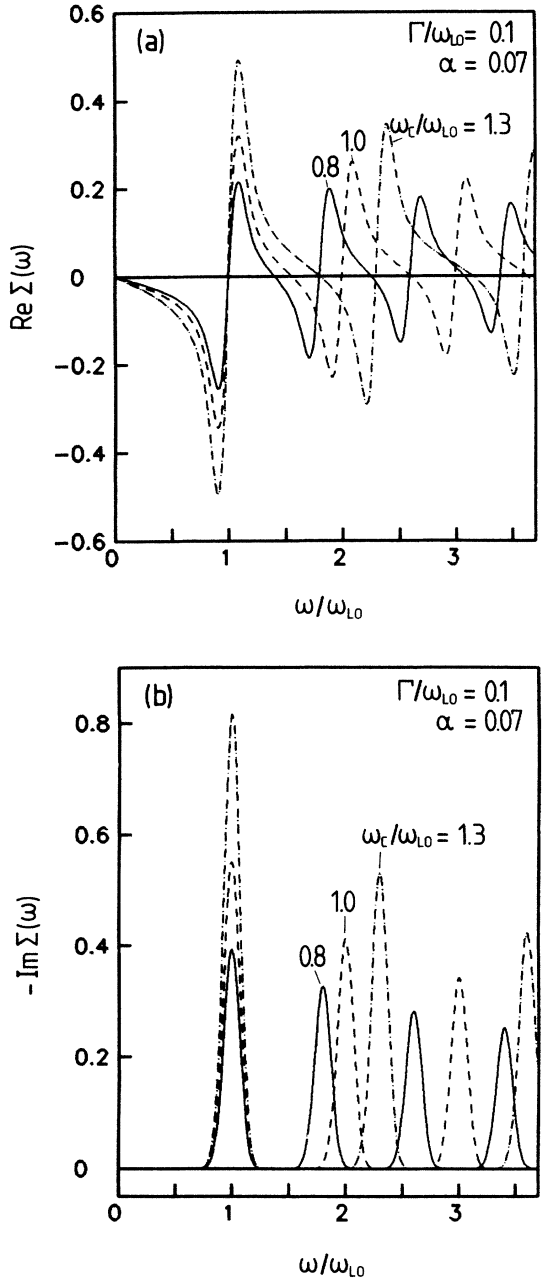

FIG. 5. (a) The real and (b) imaginary part of the memory function is plotted as function of the frequency for an ideal 2D system and for three different values of the magnetic field.

at $\omega = \omega_{\mathrm{LO}} + n\omega_c$ the dominant term in the summation of the imaginary part of the memory function [see Eqs. (9)] is, for $n \neq 0$, proportional to B_n/n, which is a decreasing function of n. The real part of the memory function, which can be obtained from the imaginary part by using the Kramers-Kronig relation, is an oscillating function. Approximately, we have $\mathrm{Re}\Sigma(\omega) = 0$ when $\mathrm{Im}\Sigma(\omega)$ attains its maximum values.

The magneto-optical absorption spectrum of the ideal 2D system for ω near ω_{LO} is plotted in Fig. 6 for different values of Γ and three values of the magnetic field strength which are chosen in such a way that they are near the resonance condition $\omega_c \sim \omega_{\mathrm{LO}}$. Similar to the case $\Gamma = 0$, we

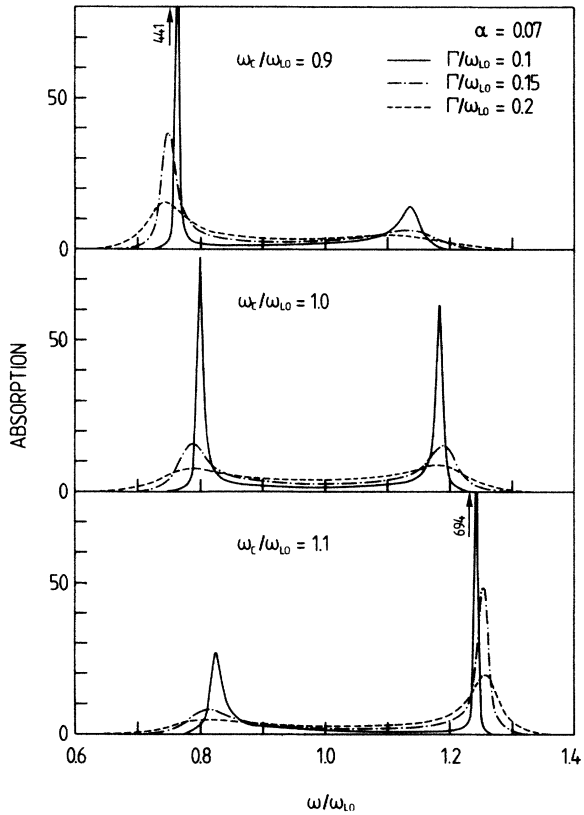

FIG. 6. The magneto-optical absorption spectrum of an ideal 2D system is shown for different values of Γ and for magentic field values around the resonance condition.

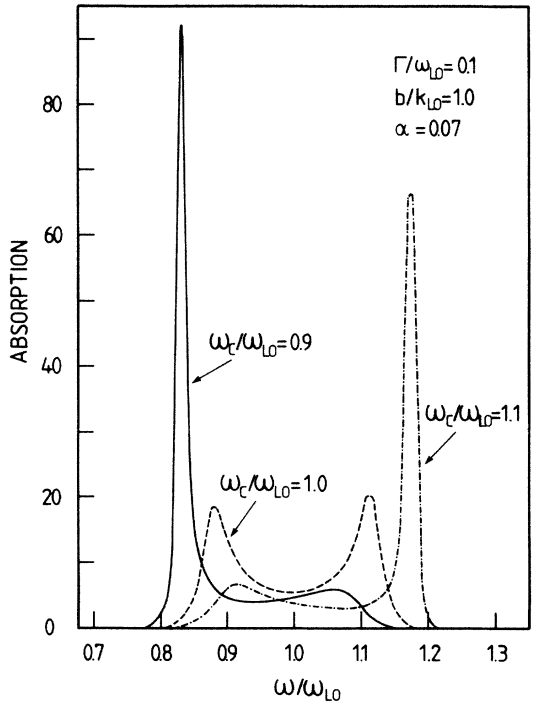

FIG. 7. The magneto-optical absorption spectrum of the Q2D system.

observe that the amplitude of the first peak decreases for increasing ω_c, while the amplitude of the second peak increases. The Landau-level broadening parameter not only affects the amplitude of the peaks but also their position. As Γ increases the peaks broaden and become less pronounced. For sufficient large Γ values the cyclotron-resonance peaks will not even be resolved. The absorption spectrum of the Q2D system is plotted in Fig. 7. The finite width of the 2D electron layer reduces the splitting of the peaks and also reduces the absorption.

The magneto-optical absorption spectrum above the LO-phonon continuum is plotted in Fig. 8 for the ideal 2D system and for different values of the magnetic field strength. The LO-phonon-assisted harmonics are clearly resolved. For a fixed magnetic field strength the amplitude of the LO-phonon-assisted harmonics decreases for higher harmonics. This is due to the fact that near the peak position ω_n one has $\omega_n \approx \omega_{\rm LO} + n\omega_c$ $(n=1,2,\ldots)$ and the amplitude of the LO-phonon-assisted harmonic peak is approximately given by $\mathrm{Im}\Sigma(\omega_n)/(\omega_n-\omega_c)^2$ [see Eq. (4)], which decreases with increasing n because also $\mathrm{Im}\Sigma(\omega_n)$ decreases with increasing ω_n [see Fig. 5(b)].

Finally in Fig. 9 we plot the splitting of the cyclotron resonance peak $(\Delta=\omega_2^*-\omega_1^*)$ at $\omega_c=\omega_{\rm LO}$ as a function of Γ, the Landau-level broadening parameter, for the ideal 2D system. As Γ increases, the splitting first increases and reaches a maximum, after which it decreases rapidly (see also Fig. 6).

IV. COMPARISON WITH EXPERIMENT

In this section we apply the theory, developed in the preceding sections, to analyze the experimental polaron cyclotron resonance data of Refs. 4 and 5 for GaAs-$Al_xGa_{1-x}As$ heterostructures and of Ref. 6 for InSb in-

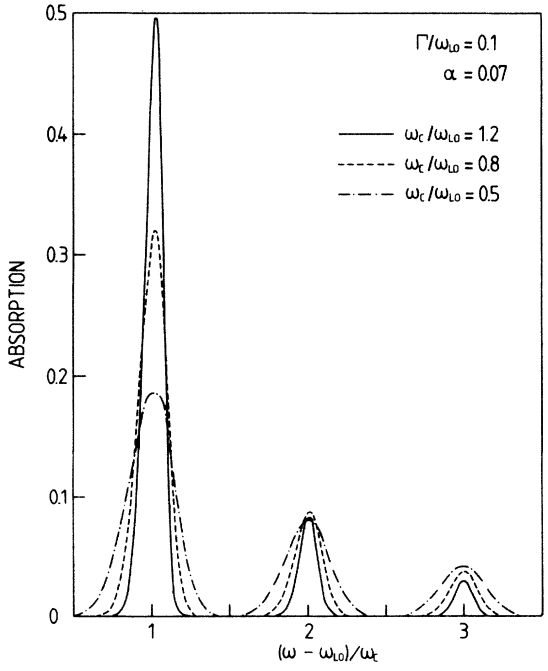

FIG. 8. The LO-phonon-assisted harmonics of the magneto-optical absorption spectrum is shown for the ideal 2D system and for different values of the magnetic field.

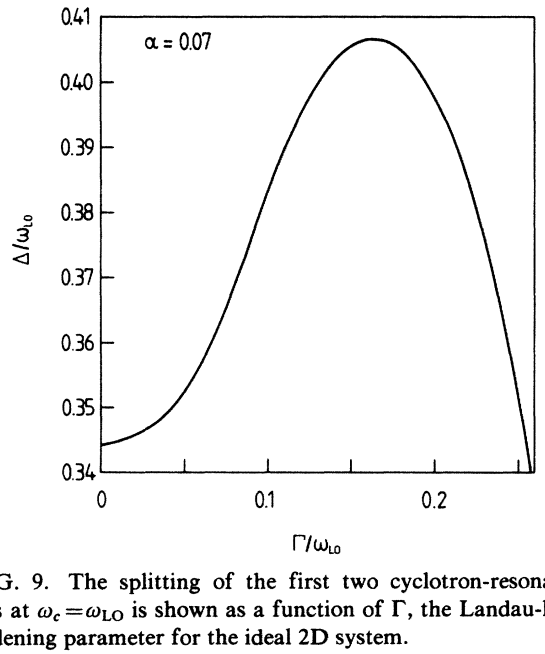

FIG. 9. The splitting of the first two cyclotron-resonance peaks at $\omega_c=\omega_{\rm LO}$ is shown as a function of Γ, the Landau-level broadening parameter for the ideal 2D system.

version layers. To make a realistic comparison with the experiments, we have to take into account the nonparabolicity of the electron energy band, which leads to an effective electron mass which increases with increasing magnetic field strength. In this respect it has a similar effect on the electron effective mass, as polaron effects have, at least when $\omega_c \ll \omega_{\rm LO}$. The essential difference between the effect of band nonparabolicity and the polaron contribution is that polaron effects induce a resonant contribution around $\omega_c \sim \omega_{\rm LO}$ which leads to a pronounced mass renormalization for these magnetic field values. This resonant behavior is absent in the case when there is only band nonparabolicity. In preceding sections energy-band nonparabolicity is neglected in the calculation of the polaron cyclotron resonance mass. In the following we will apply the theory of Zawadzki[21] in order to include the band nonparabolicity.

First, we list a few equations of Ref. 21, which will be used in this section. For details we refer to Ref. 21. In the presence of a magnetic field the energy of the electron in the lowest subband, according to Zawadzki, is given by

$$\varepsilon_{\rm np}=\varepsilon_{||}+z(\varepsilon_g+\varepsilon_{||}) , \tag{11a}$$

where z is the solution of the equation

$$\tfrac{8}{3}z^{3/2}+\tfrac{4}{5}z^{5/2}=\left[\frac{\varepsilon_g}{2m_b}\right]^{1/2}\frac{4\pi eF\hbar}{(\varepsilon_g+2\varepsilon_{||})^2}\frac{3}{4} , \tag{11b}$$

and

$$\varepsilon_{||}=-\frac{\varepsilon_g}{2}+\left[\left[\frac{\varepsilon_g}{2}\right]^2+\varepsilon_g\hbar\omega_c(n+\tfrac{1}{2})\right]^{1/2} . \tag{11c}$$

Here, ε_g is the energy band gap. F is an electric field which determines the electron-confining triangular well potential and which is treated here as a fitting parameter. In this way the electron density does not directly enter the theory. The spatial extent of the subband wave function is determined by the variational parameter b, which is given by $b=2(3eFm_b/2\hbar^2)^{1/3}$ and is consequently entirely determined by the electric field F.

Let us first consider band nonparabolicity and disregard momentarily polaron effects. The cyclotron-resonance frequency is then given by

$$\hbar(\omega_c)_{\rm np}=\varepsilon_{\rm np}(n=1)-\varepsilon_{\rm np}(n=0) ,$$

which is different from $\hbar\omega_c$. This shift from ω_c to $(\omega_c)_{\rm np}$ arises solely from the nonparabolicity of the energy band.

In the present paper we apply the following scheme in order to incorporate polaron effects together with band nonparabolicity. We use $(\omega_c)_{\rm np}$ and b, given above, as input to the equation (for convenience we take $\Gamma=0$)

$$\omega-(\omega_c)_{\rm np}-{\rm Re}\Sigma(\alpha,(\omega_c)_{\rm np},b;\omega)=0 . \tag{12}$$

The calculation of the memory function is described in Sec. II. The solution ω^* of Eq. (12) gives the cyclotron-resonance frequency, which is affected both by the nonparabolicity and by the electron-phonon coupling.

Before comparing our theoretical results with the experimental data, we discuss the physical significance of our approximations which lead to the cyclotron-resonance frequency as determined by the nonlinear equation (12). (1) Note that for (i) $\alpha=0$, i.e., in the absence of the electron-phonon interaction, Eq. (12) leads to $\omega^*=(\omega_c)_{\rm np}$, as should be the case; (ii) in the parabolic limit one has $(\omega_c)_{\rm np}=\omega_c$ and the result of preceding sections is recovered. Consequently, the correct limiting behavior is obtained if either the electron-phonon interaction or the nonparabolicity are switched off. (2) The correction to ω^* due to the band nonparabolicity and the polaron effect are not considered to be additive in Eq. (12) because (i) ReΣ also contains $(\omega_c)_{\rm np}$, and (ii) the solution of Eq. (12) denoted by ω^* results as the solution of a nonlinear equation. (3) Our approximation for the combined incorporation of the band nonparabolicity and the electron-phonon interaction corresponds to a local parabolic approximation to the band nonparabolicity. In calculating the polaron effect *all Landau levels are incorporated* in the calculation of ReΣ within this local parabolic approximation. This is in contrast to earlier work of other investigators,[5,7,21] where only the resonance term in the perturbation theory for the electron-phonon interaction was considered (see also Ref. 19). This latter approach leads to the unfortunate consequence[21] that for $\omega_c \to 0$ the cyclotron-resonance mass diverges as $m^* \sim \omega_c^{-1/2}$. This problem is not present in our approach, where the correct zero-magnetic-field limit is obtained because we sum over all Landau levels. (4) Note that in the standard calculation[4,5,7,21] the polaron cyclotron-resonance frequency is determined as the difference of two adjacent Landau levels. The Landau levels are calculated within, e.g., second-order perturbation theory. In the present approach we immediately calculate the polaron correction (see, e.g., Ref. 15), i.e., ReΣ, to the cyclotron-resonance frequency ω^* without calculating the position of the individual Landau levels. Recently, the present authors[19] showed that such an approach describes more accurately the polaron contribution to the polaron cyclotron-resonance mass. (5) The zero-temperature limit is a good

approximation to the experimental situation $T \sim 4$ K because the LO-phonon energy induces a temperature scale (i.e., $T_0 = \hbar\omega_{LO}/k_B \approx 283$ K for InSb and 426 K for GaAs), which is almost 2 orders of magnitude higher.

In comparing our theory with the experimental data, we are confronted with the problem that the value of F, or equivalently the width of the 2D electron layer, is not known experimentally. Therefore we have to take F as a fitting parameter. The nonparabolicity of the electron energy band (without polaron effect) results in a electron effective mass m^*_{np} which is almost a linear function of the magnetic field strength.[4] The incorporation of the polaron effect leads to a strong increase of the cyclotron-resonance mass m^* when $(\omega_c)_{np} \sim \omega_{LO}$ and, consequently, m^* deviates from the linear behavior of m^*_{np}. The stronger the electron-phonon coupling strength, the larger the deviation of m^* from m^*_{np}. The band mass m_b also affects m^*, but has little influence on the slope of m^* versus the magnetic field.

It is worth noticing that in the experiment of Horst *et al.* and of Sigg *et al.* the samples have almost the same electron density, i.e., $n_e = 4.07 \times 10^{11}$ and 4×10^{11} cm^{-2}, respectively. However, the polaron cyclotron-resonance mass in both experiments shows quite different behavior, particularly in the lower-magnetic-field region (see Figs. 10 and 11). This is a puzzling fact which needs more experimental attention. Therefore in the present study we will concentrate on the higher-magnetic-field region where the polaron effect is believed to be dominant. Even in the high-magnetic-field region (i.e., $H > 12$ T) the experimental results of Horst *et al.* for the cyclotron-resonance mass are slightly higher than those of Sigg *et al.*

We find that our one polaron theory cannot explain the experimental results quantitatively in the case of the GaAs-$Al_xGa_{1-x}As$ heterostructures if we use the well-known value for the electron-phonon coupling constant, i.e., $\alpha = 0.068$. For any choice for F we find that with $\alpha = 0.068$ the calculated cyclotron-resonance mass shows a rather large increase compared with the experimental data when $(\omega_c)_{np} \sim \omega_{LO}$. Therefore we will consider α as an effective electron-phonon coupling constant and adapt its value in order to fit our theory to the experiments (without confusion we will use the same notation α). The difference between this *effective* value for α and 0.068 may be interpreted as resulting from a constant overall effect of the many-particle nature of the 2D electron system on the cyclotron-resonance mass.

In Fig. 10 we plot the cyclotron-resonance mass derived from the experimental result of Horst *et al.*[4] (solid circles and solid squares) and compare it with our calculation. By using an effective $\alpha = 0.05$ and an electric field $F = 3 \times 10^4$ V/cm, we can fit our results to the experimental data when $H > 15$ T (solid curve). The electric field F results in a width of the 2D electron layer

$$\langle (z - \langle z \rangle)^2 \rangle^{1/2} = \sqrt{3}/b \approx 55 \text{ Å} .$$

The dashed curve is the result of Zawadzki.[21] We even can obtain a fitting over the whole magnetic field region (see dash-dotted curve in Fig. 10) when the effective electron-phonon coupling constant is taken as $\alpha = 0.015$,

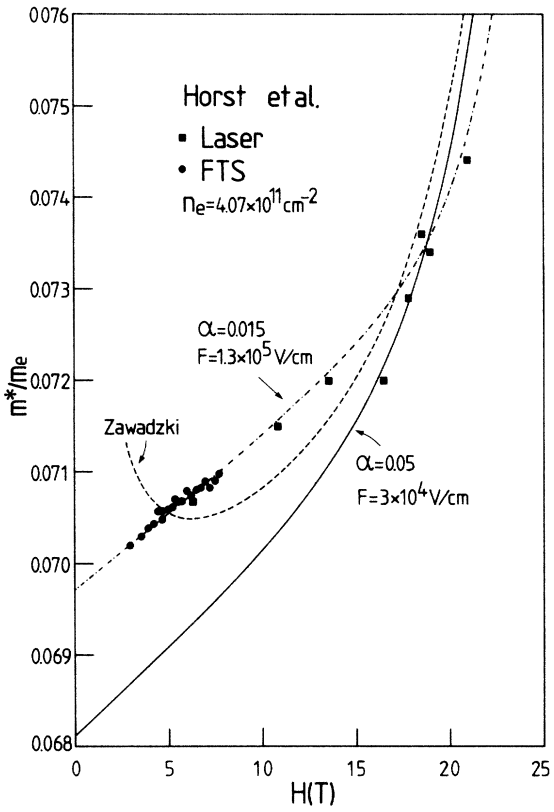

FIG. 10. The experimental data of Horst *et al.* (Ref. 4) (solid circle and square points) for GaAs-$Al_xGa_{1-x}As$ are compared with the present theoretical results (solid and dash-dotted curves). The dashed curve is the results of Zawadzki (Ref. 21). The effective electron-phonon coupling constant $\alpha < 0.068$ because many-body effects were not included.

which is about 4.5 times smaller than the well-accepted value $\alpha = 0.068$, and an electric field $F = 1.3 \times 10^5$ V/cm, which results in a very thin 2D electron layer of 34 Å.

Next, we analyze the experimental data of Sigg *et al.*[5] in Fig. 11, where we have to use an effective $\alpha = 0.05$ in order to fit the experiment in the region $H > 12$ T. This value for α is consistent with our previous one. Notice that the cyclotron-resonance mass derived from the experimental data of Ref. 5 exhibits a pronounced peak structure at $H \sim 5$ T (see Fig. 11). This is not caused by polaron effects and was attributed in Ref. 5 to a change of the filling factor from $\nu > 1$ to $\nu < 1$. Here we use a smaller electric field value $F = 2 \times 10^3$ V/cm, which leads to a electron-layer width of about 135 Å. The other physical parameters used in the calculation are $\hbar\omega_{LO} = 36.75$ meV and $\varepsilon_g = 1520$ meV. The band mass m_b is taken from Ref. 4 and is $m_b = 0.0665 m_e$.

In Fig. 12 the experimental data for InSb inversion layers[6] (for the lowest subband) are compared with our results (solid and dashed curves). The experimental data plotted as solid circles and square points correspond to the electron densities $n_e = 2 \times 10^{11}$ and 10^{12} cm^{-2}, respectively. Here we also take into account the effect of spin. For

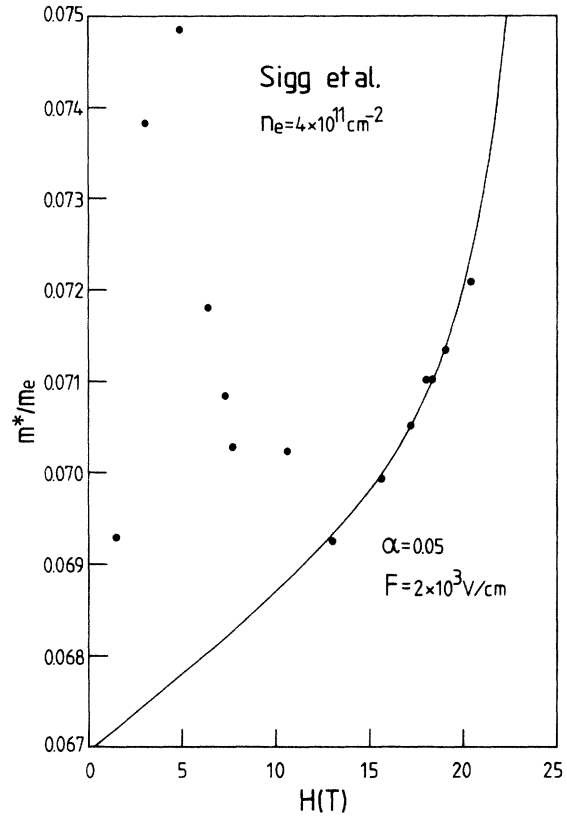

FIG. 11. The experimental results of Sigg *et al.* (Ref. 5) (solid circles) are compared with the present theoretical results (solid curve). The effective electron-phonon coupling constant $\alpha<0.068$ because many-body effects were not included.

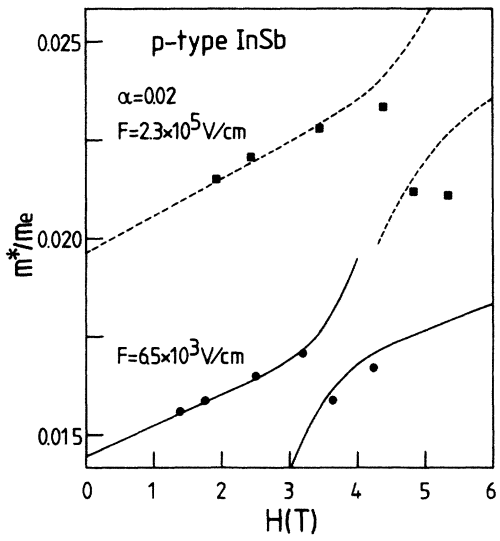

FIG. 12. The experimental data for InSb inversion layers (Ref. 6) are compared with the present theoretical results (solid and dashed curves). The solid circle and square points correspond to the experimental electron densities $n_e=2\times10^{11}$ and 10^{12} cm^{-2}, respectively.

this purpose $\hbar\omega_c(n+\frac{1}{2})$ in Eq. (11c) is replaced by $\hbar\omega_c(n+\frac{1}{2})-|g_0^*|\mu_B H/2$. The electron-phonon coupling constant is $\alpha=0.02$. The electric fields are $F=2.3\times10^5$ (two upper curves) and 6.5×10^3 V/cm (two lower curves), respectively. The other parameters are $\hbar\omega_{LO}=24.4$ meV, $m_b=0.0135m_e$, $\varepsilon_g=235$ meV, and $|g_0^*|=51$.

It is clear that the effective electron-phonon coupling strength is reduced considerably in the experiments of Refs. 4 and 5. This may be attributed to occupation effects (i.e., Fermi-Dirac statistics) and screening arising from the electron-electron interaction, which are neglected in the present study. It has been suggested in Refs. 3 and 5 that electron screening may play an important role in the electron-phonon interaction in the cyclotron-resonance experiment and may modify the polaron effects considerably. In the experiment of Ref. 3 no significant polaron effects could be identified. This can be understood by noticing the fact that the largest probe-laser energy used in the experiment is only about $\hbar\omega_{LO}/3$, corresponding to a wavelength $\lambda=96$ μm (see Ref. 3), which is far from the polaron resonance condition. Therefore the experimental results could be explained by band nonparabolicity only.

In Ref. 6 the cyclotron-resonance frequency ω^* is measured below and above the LO-phonon energy. For $\omega^*<\omega_{LO}$ the cyclotron-resonance mass m^* is almost a linear function of the magnetic field (see Fig. 12). Such a linear behavior of m^* can also be explained by band nonparabolicity. However, band nonparabolicity cannot explain the splitting of m^* for $\omega^*\sim\omega_{LO}$. The splitting of m^* in the experiment of Ref. 6 is so large that it is necessary to take $\alpha=0.02$ to explain the experimental data. $\alpha=0.02$ is the well-accepted value for the electron-phonon coupling constant in InSb. This is in contrast to the above analysis of the experimental results of Refs. 4 and 5 for the GaAs-$Al_xGa_{1-x}As$ heterostructures, where we need a smaller effective electron-phonon coupling constant to explain the data with our theory. For the moment, it is not clear why the electron-phonon coupling is not reduced in the experiment of Ref. 6 by the many-particle effects. A possibility is that occupation effects and screening are not important at the resonant condition itself.[22] Note also that in order to explain the $\omega_c<\omega_{LO}$ results of Ref. 6 no polaron effects have to be invoked.

V. CONCLUSION

In the present paper we have calculated the magneto-optical absorption spectrum of a single 2D polaron. In order to remove the divergences in the absorption spectrum we have introduced a Landau-level broadening parameter in a phenomenological way. The nonzero width of the 2D electron layer is incorporated into the memory-function calculation by considering the lowest subband. It is found that the nonzero width of the 2D electron layer considerably reduces the polaron effects. In order to make a realistic comparison between our results and the experimental data, we have taken into account the effect resulting from the nonparabolic electron energy band. When we use an *effective* electron-phonon coupling constant which is smaller than the experimentally determined

values, we are able to explain quantitatively the experimental data for GaAs-$Al_xGa_{1-x}As$ heterostructures in the high-magnetic-field region. Effects from Fermi-Dirac statistics and the electron screening are probably responsible for the reduction of the electron-phonon coupling, but this needs further theoretical consideration before we can be definite about it. We have also compared our theoretical results with the experimental data of Ref. 6 for an InSb inversion layer. We find that in this case the electron-phonon coupling constant is not reduced and that the one-polaron theory could explain the experimental results.

In the present study we have neglected the many-body effects. We have studied the problem of one polaron. Therefore the present theory is expected to be valid in the limit of low electron density only. Recently, the optical absorption spectrum of a 2D polaron has been calculated for the zero-magnetic-field case by the present authors.[23] In Ref. 23 the dynamical screening effects due to the electron-electron interaction on the electron LO-phonon interaction have been found to be important. For the Q2D electron system, like the GaAs heterostructures in Refs. 4 and 5, the electron density is not very high: $n_e \approx 4\times 10^{11}$ cm^{-2}. Near the resonance condition $\omega_c \approx \omega_{LO}$ the filling factor $\nu \leq 1$ and electrons will be in the lowest Landau level. This probably is the reason why the present one-polaron theory provides such a close agreement with the experimental results.

ACKNOWLEDGMENTS

This work is partially sponsored by FKFO (Fonds voor Kollektief Fundamenteel Onderzoek, Belgium), Project No. 2.0072.80. One of the authors (F.M.P.) acknowledges financial support from the Belgian National Fund for Scientific Research. One of us (W.X.) wishes to thank The International Culture Co-operation of Belgium for financial support. We are pleased to thank M. Horst, U. Merkt, and W. Seidenbusch for providing us with their experimental data and H. Sigg for interesting discussions.

*Also at University of Antwerp (RUCA), B-2020 Antwerpen, Belgium, and Eindhoven University of Technology, NL-5600 MB Eindhoven, The Netherlands.

[1] *Polarons and Excitons,* edited by C. Kuper and G. Whitfield (Oliver and Boyd, Edinburgh, 1963); *Polarons in Ionic Crystals and Polar Semiconductors,* edited by J. T. Devreese (North-Holland, Amsterdam, 1972); *Polarons and Excitons in Polar Semiconductors and Ionic Crystals,* edited by J. T. Devreese and F. M. Peeters (Plenum, New York, 1984).

[2] T. Ando, A. B. Fowler, and F. Stern, Rev. Mod. Phys. **54**, 437 (1982).

[3] W. Seidenbusch, G. Lindemann, R. Lassnig, J. Edlinger, and G. Gornik, Surf. Sci. **142**, 375 (1984).

[4] M. Horst, U. Merkt, W. Zawadzki, J. C. Maan, and K. Ploog, Solid State Commun. **53**, 403 (1985).

[5] H. Sigg, P. Wyder, and J. A. A. J. Perenboom, Phys. Rev. B **31**, 5253 (1985).

[6] M. Horst, U. Merkt, and J. P. Kotthaus, Phys. Rev. Lett. **50**, 754 (1983).

[7] R. Lassnig and W. Zawadzki, Surf. Sci. **142**, 388 (1984).

[8] S. Das Sarma and A. Madhukar, Phys. Rev. B **22**, 2823 (1980).

[9] D. Larsen, Phys. Rev. B **30**, 4595 (1984).

[10] F. M. Peeters and J. T. Devreese, Phys. Rev. B **31**, 3689 (1985); F. M. Peeters, Wu Xiaoguang, and J. T. Devreese, *ibid.* **33**, 4338 (1986).

[11] S. Das Sarma, Phys. Rev. Lett. **52**, 859 (1984); **52**, 1570(E) (1984).

[12] D. Larsen, Phys. Rev. B **30**, 4807 (1984).

[13] J. Van Royen, J. De Sitter, L. F. Lemmens, and J. T. Devreese, Phys. Physica **81B**, 101 (1977); J. P. Vigneron, R. Evrard, and E. Kartheuser, Phys. Rev. B **18**, 6930 (1978); J. Van Royen, J. De Sitter, and J. T. Devreese, *ibid.* **30**, 7154 (1984); F. M. Peeters and J. T. Devreese, Physica **127B**, 408 (1984).

[14] W. Götze and P. Wölfe, Phys. Rev. B **6**, 1226 (1972).

[15] F. M. Peeters and J. T. Devreese, Phys. Rev. B **28**, 6051 (1983).

[16] J. T. Devreese, J. De Sitter, and M. Goovaerts, Phys. Rev. B **5**, 2367 (1972).

[17] R. R. Gerhardts, Z. Phys. B **21**, 275 (1975); **21**, 285 (1975).

[18] R. P. Feynman, R. W. Hellwarth, C. K. Iddings, and P. M. Platzman, Phys. Rev. **127**, 1004 (1962).

[19] F. M. Peeters, Wu Xiaoguang, and J. T. Devreese, Phys. Rev. **34**, 1160 (1986).

[20] S. Das Sarma, Phys. Rev. B **27**, 2590 (1983); **31**, 4034(E) (1985); Wu Xiaoguang, F. M. Peeters, and J. T. Devreese, Phys. Status Solidi B **133**, 229 (1986).

[21] W. Zawadzki, Solid State Commun. **56**, 43 (1985).

[22] M. Horst, U. Merkt, and K. G. Germanova, J. Phys. C **18**, 1025 (1985).

[23] Wu Xiaoguang, F. M. Peeters, and J. T. Devreese, Phys. Rev. B **34**, 2621 (1986).